Reac Kinet Mech Cat (2013) 110:459–470
DOI 10.1007/s11144-013-0599-5

Effect of structural defects in alumina supports on the formation and catalytic properties of the active component of reforming catalysts

Ella M. Moroz · Dmitriy A. Zyuzin · Valentina Yu. Tregubenko · Irina E. Udras · Alexander S. Belyi · Vladimir A. Likholobov

Received: 29 March 2013 / Accepted: 27 June 2013 / Published online: 12 July 2013

Abstract The pair distribution function (PDF method) was used to investigate the phase composition and local structure of supports and the model reforming catalysts Pt/γ-Al_2O_3. The structural modification of support during acidic peptization of aluminum hydroxide with the pseudoboehmite structure was suggested as a possible approach to obtaining highly defective alumina. This modification of γ-Al_2O_3 results in the formation of a greater number of cation vacancies in the octahedral positions of the spinel-like alumina structure. The effect of structural defects in the support on the oxidation state of the active component and catalytic properties of the catalysts was demonstrated. It was found that platinum ions are located in the vacant octahedral positions (defects) of the spinel-like structure of the support. These ionic platinum centers on alumina with higher defect density demonstrated a higher selectivity in the model reaction of *n*-heptane aromatization as compared to metallic centers which prevail in traditional Pt/γ-Al_2O_3 catalyst.

Keywords Platinum catalyst · Defects of γ-alumina · PDF method · Reforming

Introduction

Reforming catalysts are commonly based on the Pt/γ-Al_2O_3 system [1]. The dispersion and charge states of the active catalyst component are determined by the physicochemical properties of the support; thus, the selection and synthesis of substrates for supported catalysts are important steps in catalyst preparation.

E. M. Moroz · D. A. Zyuzin
Boreskov Institute of Catalysis SB RAS, Lavrentieva Str. 5, 630090 Novosibirsk, Russia

V. Yu. Tregubenko (✉) · I. E. Udras · A. S. Belyi · V. A. Likholobov
Institute of Hydrocarbons Processing SB RAS, Neftezavodskaya Str. 54, 644040 Omsk, Russia
e-mail: kalinina_ihcp1@mail.ru

The γ-Al_2O_3 structure is generally considered to be a defect spinel (AB_2O_4) with four molecules in a unit cell [2, 3]. In such a structure, oxygen anions form a dense cubic packing with octahedral and tetrahedral hollows being partially occupied by aluminum cations. A crystal unit cell of γ-Al_2O_3 is represented by the structural formula $A_8[B_{13.33}\square_{2.66}]O_{32}$, where 8 aluminum cations are located in the tetrahedral positions of the spinel structure, 13.33 are located in octahedral positions, and 2.66 hollows are vacant. Cation vacancies can be considered to be defects of the spinel structure. Additionally, defects of the γ-Al_2O_3 structure are also introduced by a disordered arrangement of aluminum cations, chiefly in the octahedral positions of the spinel structure. Structural defects typically emerge in γ-Al_2O_3 following the high-temperature calcination of aluminum hydroxide, which is the oxide precursor [4]. According to [5, 6], alumina has a spinel-like structure, which is described by the more general formula, $A^*_{x1}A_{x2}[B^*_{y1}B_{y2}]O_{32-z}(OH)_z$, where **A*, B*** and **A, B** are the nonspinel and spinel positions of cations in the oxide structure; $\mathbf{x_1}$, $\mathbf{y_1}$ and $\mathbf{x_2}$, $\mathbf{y_2}$ are their amounts.

Current proposals for the arrangement of face-centered cubic metals on the γ-Al_2O_3 surface [7] suggest that platinum particles in alumina-platinum catalysts are epitaxially bound to the surface of the support, with their {111} faces adjoining the surface. During synthesis, the deposition of platinum complexes is accompanied either by exchange with the surface OH groups of the support or by the insertion of platinum ions into the defect vacancy sites of γ-Al_2O_3. Furthermore, anionic exchange of the surface OH^- groups and $[PtCl_6]^{2-}$ results in the formation of platinum complexes. These complexes are weakly bound to the support and are readily reduced to the metallic Pt^0 state. The interaction of metal complexes and alumina via this coordination mechanism involving ligand substitution in the coordination sphere of platinum leads to the formation of $PtCl_xO_y$ surface compounds [8]. In this case, due to strong interaction with the support, platinum is in the electron deficient (ionic) state with platinum(II) complexes incorporated in the surface layers of alumina at the defect sites [9]. Data on the ionic state of platinum in alumina-platinum catalysts were first reported in [10] and then verified by others [5, 11]. Modern ideas on the structure of platinum catalysts dictate an essential role for ionic platinum species in catalyzing the transformation of hydrocarbons [12]. Such ionic platinum species show an order of magnitude higher atomic activity towards the aromatization of *n*-alkanes when compared with disperse Pt^0 [13].

Properties of the nascent active component can be controlled by the deliberate synthesis of defects in the support structure. The structural modification of γ-Al_2O_3 during peptization of aluminum hydroxide with the pseudoboehmite structure was suggested as a possible approach to obtaining highly defective alumina. Mineral and/or organic acids are introduced to aluminum hydroxide to yield basic aluminum salts on the surface of primary AlOOH particles [14–16]. Thermal decomposition upon calcining in an oxidative atmosphere produces a greater number of defects [17]. The resulting oxide possesses structural and adsorption characteristics differing from those of non-peptized γ-Al_2O_3 [17, 18].

The aim of the work was to reveal specific features of the formation of the active component in alumina-platinum catalysts supported on aluminum oxides with

varying amount of structural defects and to investigate the catalytic properties of the catalysts with such supports.

Experimental

Preparation of γ-Al_2O_3 supports

The hydroxide (pseudoboehmite phase) was obtained by continuous cold deposition using admixtures containing Fe (0.012 wt%) and Na_2O (0.004 wt%) as the γ-Al_2O_3 precursor.

The (H-1) support was prepared by peptization of pseudoboehmite using a solution of nitric acid (1.5 wt% relative to the support weight) or oxalic acid (10 wt%) for the (H-2) sample. The resulting material had a moisture content of 58 % and formed as extrudates 1.5 mm in diameter. The aluminum hydroxide was dried at room temperature for at least 3 h, and then at 120 °C in a drying oven for 1 h. The support was calcined in a muffle furnace by flowing dry air over the sample at 630 °C for (H-1) and at 520 °C for (H-2), with 1 h of holding time at the final temperature. The calcination temperature was chosen to provide a complete decomposition of aluminum salts in a flow of dry air.

Preparation of K̀H-1 and K̀H-2 catalysts (2.0 wt% Pt/Al_2O_3)

Platinum was deposited using H_2PtCl_6 via the adsorption impregnation on a chlorinated alumina surface to realize coordination mechanism involving ligand substitution in the coordination sphere of platinum [8]. A freshly calcined support (extrudates) was evacuated for 10 min to a residual pressure of 10^{-2} Torr. The support was washed with water and then treated with a solution of hydrochloric acid (2.5 wt% Cl^- relative to the support weight) with both cold (25 °C) and hot (75 °C) impregnation for 30 min. Next, the solution was removed from the flask, the support was washed with distilled water, and a calculated solution of H_2PtCl_6 (C = 28.2 mg/ml) was added in several portions with vigorous stirring with cold (25 °C) impregnation for 30 min and hot (75 °C) impregnation for 1 h. The indicated duration of treatment provided sorption of the bulk of the metal complex without noticeable dissolution of alumina in the acidic medium. After the impregnation, the solution was removed and catalysts were dried at 120 °C in a drying oven for 1 h. The catalysts were calcined for 5 h in a glass reactor at atmospheric pressure in a flow of dry air upon temperature elevation to 500 °C and held at this temperature for 1 h. Reduction of the samples was performed at the same reaction vessel with flowing hydrogen at 500 °C for 1 h. During X-ray examination, the samples were not protected from air.

X-ray diffraction and structural analysis

XRD patterns of the synthesized supports were obtained on a DRON-3 diffractometer using CuK_α radiation. Experimental data for calculating the radial

electron density distribution curves (PDF) were collected on a high-resolution diffractometer at the Siberian Synchrotron and Terahertz Radiation Center using a diffraction beam with a Si (111) monochromator that generates radiation with wavelength $\lambda = 0.6987$ Å and provides monochromatization of $\Delta\lambda/\lambda \sim 10^{-4}$. Data collection covered a in the 2θ angle range of 5–135°. PDF curves of the samples were calculated by a technique reported by Moroz et al. [5, 19, 20] and then compared with the model curves for γ-Al_2O_3 presented in [6, 19]. Considering the possible formation of oxide phases upon exposure of the catalysts to air, we plotted model curves for $H_2Pt(OH)_6$ crystal phases and various platinum oxides using structural data from the ICSD/Retrieve database [21]. Interatomic distances and coordination numbers were calculated using the ICSD/Retrieve program.

Adsorption porosimetry and pycnometry

Parameters characterizing the porosity were determined from the nitrogen adsorption–desorption isotherms at −195.7 °C obtained using a Sorptomatic-1900 instrument (Carlo Erba). Specific BET surface area (S_{BET}) was calculated in the range of equilibrium using relative values of nitrogen vapors of $P/P_S = 0.05-0.33$ from adsorption isotherms. The total adsorption pore volume ($V_{\Sigma pore}$) was determined from the nitrogen adsorption at $P/P_S = 0.996$, where the density of adsorbed nitrogen taken equal to that of normal liquid (molar volume of liquid N_2 is 34.68 cm^3/mol).

The real density of the alumina samples was measured by helium pycnometry (ρ_{He}, g/cm^3) using an AccuPyc-1330 instrument (Micromeritics). The measurement accuracy for this series of samples was ±0.002 g/cm^3.

Adsorption measurements

The dispersity of the reduced platinum particles was measured by the oxygen-hydrogen titration method [22].

The application of the original adsorption technique [22] allowed us to make quantitative determination of the surface platinum atoms in different oxidation states in the supported catalysts: ionic platinum Pt^{σ} with an the oxidation state close to that found for platinum in chloride complexes, and metallic platinum Pt^0. This method is based on the ability of ionic platinum to form strong σ-donor bonds with water at relative pressures of $P/P_S < 0.05$. For the supported catalysts, quantification of the surface platinum atoms in different states was estimated from oxygen chemisorption on a pure platinum surface and only at metallic sites when ionic platinum sites are blocked by pre-adsorbed water.

Catalytic activity test

The catalysts were tested using a model reaction of *n*-heptane reforming using an isothermal plug-flow reactor at temperatures between 460 and 520 °C, a pressure of 0.1 MPa, volume feed rate of the raw material ranging from 8 to 14 h^{-1} and a hydrogen to hydrocarbon ratio of 5:1 (mol). The compositions of the resulting

hydrocarbon product mixtures were analyzed on line with the use of a gas chromatograph equipped with a capillary column and a flame-ionization detector.

Results of the testing were used to calculate the rate constants for the two main routes of *n*-heptane transformation (aromatization—k_a, cracking—k_c). The selectivity of aromatization (S) was found as a k_a/k_t ratio, where k_t is the total rate constant for *n*-heptane transformation. The activation energy was calculated from the data of catalytic experiments at temperatures of 460, 480, 500 and 520 °C.

Results and discussion

Phase composition and textural characteristics

Al_2O_3 supports

Phase composition and structural and textural characteristics of the tested supports are listed in Table 1.

As shown in Table 1, samples of the alumina supports are present in the γ-form with virtually identical unit cell parameters and sizes of their coherent scattering domain (CSD). The values of specific surface areas and pore volumes of the samples indicate a well-developed porous structure. X-ray density of the samples are similar, but exceed the density measured by helium pycnometry. Sample (H-2), obtained from the hydroxide peptized with oxalic acid, has a lower density according to helium pycnometry. It is known that, for the majority of porous solids, helium pycnometry density can be considered as the real density, which is usually calculated from X-ray structural data for single crystals [23]. Real density is a constant physical characteristic of the material, which cannot be altered without changes in its chemical composition or molecular structure. The phase and chemical compositions of the tested samples are identical and therefore, it is presumed that observed differences result from changes in the molecular structure of the two alumina supports.

During the peptization, the hydroxide interacts with the introduced acids to form aluminum salts on the surface of primary particles, which rapidly hydrolyze in an aqueous medium. This process is accompanied by disaggregation of aluminum hydroxide secondary particles and by a more close packing of the primary particles. Calcination in flowing air results in the decomposition of basic aluminum salts and

Table 1 Structural characteristics and parameters of the porous structure of supports

Sample	Phase composition	Structural characteristics			Porous structure parameters			
		Unit cell parameter (nm)	CSD (nm)	$\rho_{X\text{-}ray}$ (g/cm^3)	S (m^2/g)	V (cm^3/g)	D (nm)	ρ_{He} (g/cm^3)
H-1	γ-Al_2O_3	0.7915	5.0	3.354	218	0.70	12.75	3.262
H-2	γ-Al_2O_3	0.7919	4.5	3.349	266	0.65	9.8	3.176

transformation of the hydroxide into oxide. Basic aluminum oxalate decomposes in the temperature range of 200–400 °C. The gas-phase decomposition products include only CO, CO_2 and H_2O, which are evidence of full decomposition of organic salts [18, 24]. Nitric acid salts decompose at higher temperatures, up to 600 °C [25]. In both cases, the decomposition of the aluminum salts and removal of the gas-phase decomposition products leads to the formation of anionic vacancies (defects) on the surface of alumina primary particles. In the process, coordinatively unsaturated Lewis acidic aluminum atoms (Al^{3+}) appear at the surface [26]. According to IR spectroscopy of adsorbed CO [17], calcination of the hydroxides peptized with organic acids produces a greater number of vacancies in oxides as compared to the sample synthesized from non-peptized hydroxide. The increase in the number of vacancies is accompanied by an increase in the number of Lewis acidic sites. Additionally, the formation of anionic vacancies leads to general disordering of the structure, in particular, of the cationic framework of the alumina [4]. Changes in the molecular structure show up as changes in the local structure of the supports and affect the helium pycnometry density, which may thus serve as a criterion of support defect density.

In this context, it follows from Table 1 that (H-2), which was synthesized from pseudoboehmite peptized with oxalic acid, has a more defective structure. The greater defect density in its structure may be related to two concurrent processes that take place at the same temperature: the decomposition of basic aluminum oxalate and the transformation of hydroxide into oxide. The decomposition of basic aluminum nitrate proceeds at a temperature higher that 600 °C after the formation of a stable γ-Al_2O_3 structure. Along with changes in the helium pycnometry density ρ_{He}, the specific surface area of (H-2) increases, whereas the pore volume and diameter of (H-2) decrease (Table 1).

Pt/γ-Al_2O_3 catalysts

After the impregnation of the samples with a platinum-containing solution and subsequent thermal activation, the parameters characterizing the porous structure of the supports remain virtually unchanged. The Cl^- amount after treatment is 1.5 wt% for both catalysts. As shown by XRD, the catalyst samples are free of the crystallized phase of metallic platinum with CSD above 5 nm, as no diffraction peaks of this phase were observed in the angle range $2\theta = 39.76°$; 46.24°; 67.45°. This implies that the supported platinum does not manifest itself as an ordered, crystallized phase, but rather is highly dispersed or is present in the ionic form in the support. Additional information on the phase composition and local structure of the supports and Pt/Al_2O_3 catalysts were obtained using the PDF method.

Determination of the local structure

γ-Al_2O_3 supports

Due to the unique structural features of the tested materials and uncertainty associated with the PDF measurements, our diffraction experiment data may differ

slightly from structural data for known phases. In this context, it becomes necessary to compare experimental PDF curves with the model curves plotted for an expected phase composition [19, 20]. This may not only refine the phase composition (for X-ray amorphous and finely dispersed materials) but may also reveal structural features of the phases present in the material. We compared experimental PDF curves with the model curves plotted for the suggested phase composition of the samples. We used the data obtained and reported previously by Moroz et al. [19] to model PDF curves for γ-Al_2O_3 with "partial" curves fit for different phases representing the contribution of individual groups of interatomic distances.

Fig. 1 shows the experimental PDF curves of the tested supports (H-1) and (H-2), which were calculated by a similar procedure from experimental diffraction data obtained under identical conditions. Differences in the local structure of supports are most pronounced in the region of r = 3.3, 4.5, 5.1, 5.9, 6.4, 7.5 Å. These interatomic distances correspond to the distances between cations in tetrahedral (A) and octahedral (B) positions of a dense oxygen packing (distances A–A and A–B) and to the oxygen-cation distances (O–B). As follows from Fig. 1, areas of the first coordination sphere are similar for both samples, whereas differences are observed in the outer spheres. A decrease in the areas of coordination peaks in the PDF curve of (H-2) in comparison with the curve for (H-1) is attributed to a lower filling of octahedral positions, which points to the formation of a greater number of cation vacancies in the structure of (H-2).

A previous PDF study [20] revealed the presence of isolated sections on the surface of the spinel-like alumina phase where octahedral vacancies are occupied by platinum ions, which are the formation sites for disperse zero valent platinum. It has been demonstrated [8, 9] that due to a strong interaction with the support, the platinum is present as complexes of platinum(II) built into the surface layers of the alumina at the sites of its structural defects. In this case, the active component will form differently on supports with different local structures. The higher surface area

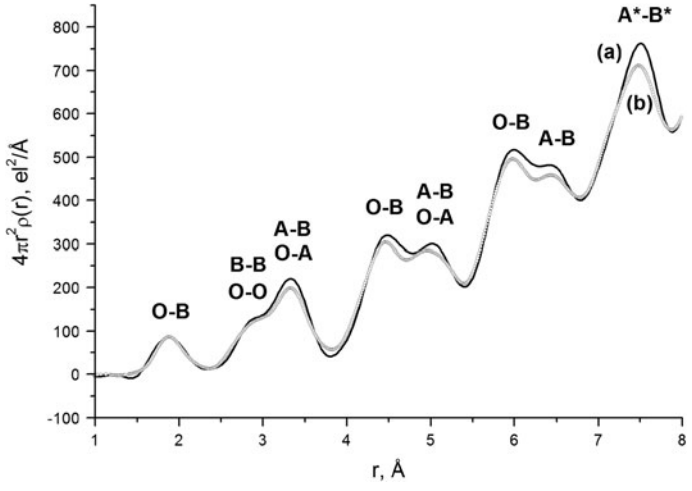

Fig. 1 Experimental PDF curves of alumina with ρ_{He} = 3.262 g/cm^3 (**a**) and ρ_{He} = 3.176 g/cm^3 (**b**)

and greater number of unoccupied octahedral positions in the structure of (H-2) should lead to a higher ionic platinum content in the catalyst and a more uniform distribution of zero valent platinum.

Pt/γ-Al_2O_3 catalysts

It is difficult to analyze the overall PDF curve of the catalyst, as it includes not only distances typical of the support and active component structure, but also new coordination peaks related to interatomic distances corresponding atoms of the support with atoms of the active component. Thus, to provide a more comprehensive characterization of the catalyst structure, the difference PDF curves are used (the curve of the support alone is subtracted). It is assumed that at a low concentration of active component, the PDF curve of the support is present in the catalyst curve in its unaltered form [27, 28].

According to [5, 29], in the case of supported metal catalysts, the difference PDF curve may be used to get information on the active component phase (from a typical set of interatomic distances), to estimate its abundance and CSD size (by comparing the peak areas of experimental PDF curves with the areas on calculated curve), and to reveal the interaction phase (from the appearance of new interatomic distances and a decrease in the areas of coordination peaks corresponding to the metallic phase). Such information considerably extends the knowledge of the phase composition, dispersity and structure of the supported catalyst.

Figs. 2 and 3 show the difference PDF curves of the tested catalysts (in each case the respective support was subtracted). It can be seen from these data that the local structure of the catalysts is different. First, interatomic distances typical of metallic platinum (r = 2.77, 3.92, 4.80, 5.55 Å) are not observed in the catalysts. On the difference curve of (ḰH-1), the catalyst reduced at 500 °C (Fig. 2), there are coordination peaks corresponding to PtO_2 and $H_2Pt(OH)_6$. These phases may form upon contact with air of the reduced sample, which contains highly dispersed particles of metallic platinum. The $H_2Pt(OH)_6$ phase corresponds to distances r = 2.15, 3.71, 4.15 and 5.17 Å (Pt–O and Pt–Pt distances in this phase). A group of coordination peaks in the region of r = 3–3.5, 4.2–4.5, 4.85, 5.4, 5.9 Å belongs to Pt–Pt and Pt–O distances in the structure of platinum oxide PtO_2. A peak in the region of r = 2.5 Å corresponding to the Pt–Cl bond within the $PtCl_6^{2-}$ anion [29]. We assign this correlation to the Pt–Cl bond which is an expected to be interaction of the particles with the surface of the support.

The situation is different for (ḰH-2), the catalyst prepared using the (H-2) support (Fig. 3). Although the curve of the support was subtracted, the difference PDF curve of this catalyst still has coordination peaks corresponding to B–B, A–B and O–B distances of the spinel-like phase. These peaks may belong to distances in the surface clusters, which comprises platinum ions located in the vacant octahedral positions of the spinel-like structure of the support. These clusters form on the surface of the support during its impregnation with a solution of chloroplatinic acid and at subsequent steps of oxidative and reductive treatments. Platinum ions form due to an incomplete reduction of metal complexes [13, 27]. The nascent cluster is characterized by distances typical of the spinel-like structure: in the region of

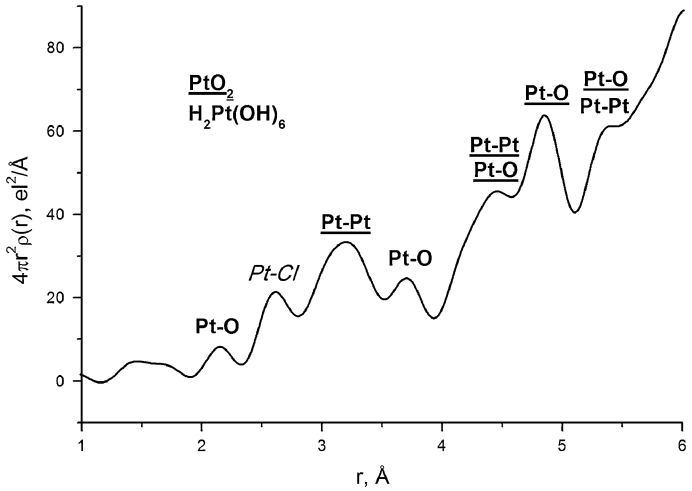

Fig. 2 Difference PDF curve for catalyst KH-1

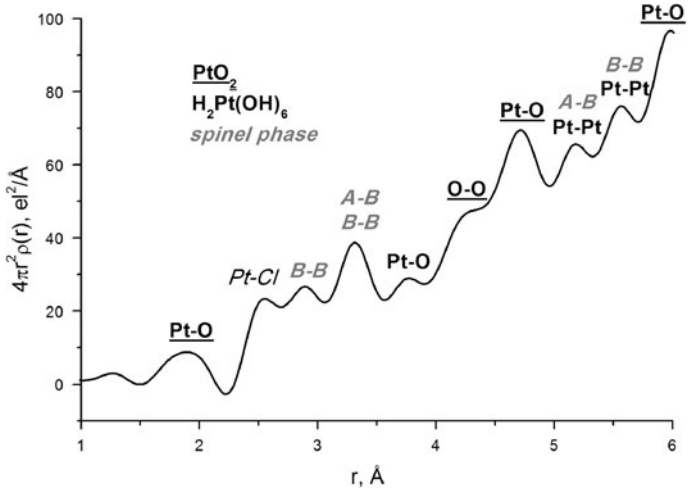

Fig. 3 Difference PDF curve for catalyst KH-2

r = 2.89, 3.31, 4.64, 5.57 Å (B–B distances), in the region of r = 3.31, 5.18 Å (A–B distances), and in the region of r = 1.98, 3.42, 4.42, 5.93 Å (B–O distances). There is a peak in the region of r = 2.5 Å in the PDF of the catalyst (KH-2) treated in hydrogen at 500 °C. We assign this correlation to the Pt–Cl bond [29] which is an expected to be interaction of the particles with the surface of the support. The presence of platinum oxide PtO_2 cannot be excluded for this sample. The distance r = 3.77 Å may be assigned to Pt–O bond in the structure of $H_2Pt(OH)_6$; Pt–Pt distances with r = 5.18, 5.57 Å are also typical of this phase. Judging from the relative amount of the PtO_2 phase present, the amount of dispersed metallic

platinum is greater in the catalyst whose support has a smaller number of defects and hence a lower amount of ionic platinum, i.e., in the (ḰH-1) sample.

Testing of catalytic properties

The phase composition of the active component affects the overall catalytic behavior. A typical model reaction for testing the catalytic properties of supported platinum is aromatization of *n*-heptane (460–520 °C). Such testing revealed the effect of support structure and features of the active component on catalytic properties of these materials. The study was performed with samples of alumina-platinum catalysts having a metal concentration of 2.0 wt%. Prior to chemisorption and catalytic measurements, the samples were precalcined at 500 °C and reduced at the same temperature. Data on the dispersity of platinum obtained by O_2–H_2 titration are listed in Table 2. It is seen that catalysts have close dispersity of the active component. However, the (ḰH-2) sample (with a more defective support) contains a greater concentration of ionic platinum. Thus, adsorption data agree with the PDF data on the oxidation state of the active component in the catalysts.

Fig. 4 shows data on the catalytic activities of the tested samples. At similar aromatization activity (Fig. 4a), the number of sites on which the target reaction takes place (Fig. 4b) is noticeably greater for the sample prepared using the support having a greater defect density. The (ḰH-2) catalyst demonstrated a higher selectivity (Fig. 4b) in the model reaction of *n*-heptane aromatization as compared to (ḰH-1), which can be attributed to differences in the state of the active component in the tested samples. (ḰH-1) has a greater amount of dispersed metallic platinum, while in (ḰH-2), the ionic form of platinum prevails.

It is known that Cl^- in alumina and in catalyst increases acidity of these materials and influences on catalytic properties of Pt/Al_2O_3 systems decreasing selectivity of *n*-heptane aromatization [1]. Both catalysts (KH-1 and KH-2) contain similar amounts of Cl^- after treatment, so the differences in catalytic testing can be attributed to the role of number of alumina defects in the Pt phase formation.

Thus, the use of supports with different structural defect densities led to the formation of platinum sites differing in their adsorption and catalytic properties. The strong interaction of platinum with the highly defective support prevents a complete reduction of the metal, which leads to the stabilization of ionic Pt species that determine high efficiency of the catalyst for *n*-heptane aromatization.

Table 2 Characteristics of the catalyst active component

Sample	Platinum dispersity (%)	Amount of surface Pt (μmol/g_{cat})	
		Pt^{σ}	Pt^{o}
ḰH-1	69	48	23
ḰH-2	65	56	11

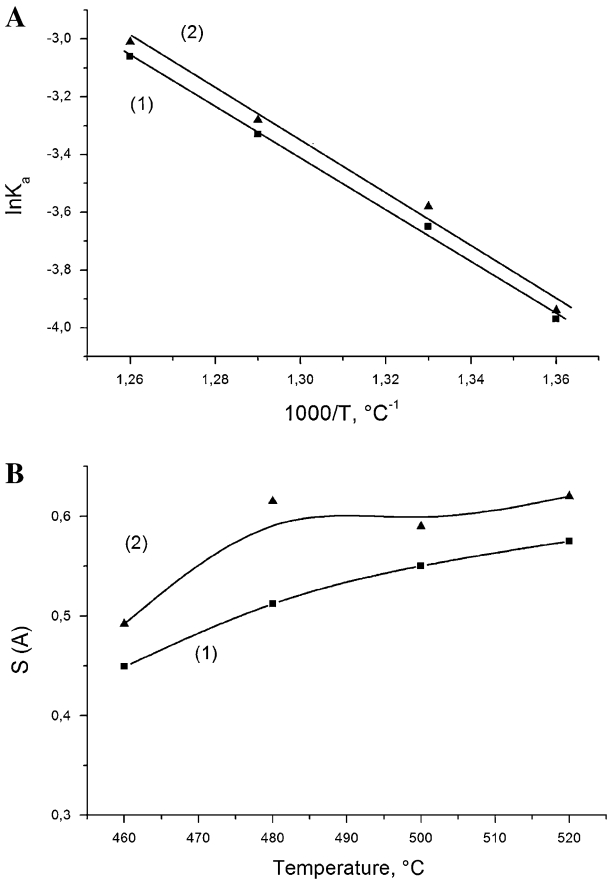

Fig. 4 A comparison of 2.0 wt% Pt/Al_2O_3 samples ḰH-1 (*1*) and ḰH-2 (*2*) in *n*-heptane aromatization: **a** aromatization constant versus the reaction temperature; **b** selectivity of aromatization versus the reaction temperature

Conclusions

A support synthesized from the hydroxide peptized by oxalic acid was found to have a higher defect density, which manifests itself in the formation of a greater number of cation vacancies in octahedral positions of the spinel-like alumina structure according to PDF data. The similar amounts of Cl^- in the catalysts whose support has a greater number of vacancies show that there are a greater number of the "interaction clusters" formed with ionic platinum and a smaller amount of metallic platinum. The catalyst synthesized with a more defective support has a higher selectivity in *n*-heptane aromatization.

Acknowledgments The authors are grateful to A.N. Shmakov for synchrotron radiation experiments and E.A. Belopukhov for interest in manuscript preparation. The work was supported by RFBR (Project No. 09-03-90424).

References

1. Antos GJ, Aitani AM, Parera JM (1995) Catalytic naphtha reforming, science and technology. Marsel Dekker, New York
2. Knozinger H, Ratnasamy P (1978) Catal Rev Sci Eng 17:31–70
3. Gutiérrez G, Johansson B (2001) Phys Rev B: Condens Matter Mater Phys 65:104202
4. Paglia G, Bozin ES, Billinge SJL (2006) Chem Mater 18:3242–3248
5. Moroz EM (2011) Russ Chem Rev 80:315–334
6. Moroz EM, Zuzin DA, Shefer KI, Isupova LI (2007) Russ J Struct Chem 48:754–756
7. Moroz EM, Pakharukova VP, Shamkov AN (2009) Nucl Instrum Methods Phys Res, Sect. A 603:99–101
8. Belskaya OB, Duplyakin VK (2007) Ross Khim Zh 51:754–763
9. Belyi AS, Smolikov MD, Kiryanov DI, Udras IE (2007) Ross Khim Zh 77:2243–2254
10. McHenry KW, Bertolachini RJ, Brennan HM, Wilson JL (1961) Proceedings of the II International congress on catalysis. France, Paris, pp 2295–2311
11. Escard J, Pontviannt R, Chenebaux MT, Cosyns J (1976) Bull Soc Chim France 3–4:349–354
12. Shi H, Gutiérrez OY, Yang H, Browning ND, Haller GL, Lercher JA (2013) Am Chem Soc Catal 3:328–338
13. Belyi AS (2008) Kinet Catal 49:562–567
14. Dzis'ko VA, Karnaukhov AP, Tarasova DV (1978) Physicochemical bases for synthesis of oxide catalysts. Nauka, Novosibirsk
15. Dzis'ko VA (1983) Fundamentals of catalyst preparation methods. Nauka, Novosibirsk
16. Jiratova K, Janacek L, Schneider P (1983) In: Poncelet G, Orange P, Jacobs PA (eds) Preparation of catalysts III. Elsevier, Amsterdam
17. Tregubenko VYu, Udras IE, Drozdov VA, Belyi AS (2009) Russ J Phys Chem A 83:2039–2044
18. Tregubenko VYu, Udras IE, Belyi AS (2009) Kinet Catal 50:878–879
19. Moroz EM, Zuzin DA, Shefer KI (2007) J Struct Chem 48:262–269
20. Pakharukova VP, Moroz EM, Zuzin DA (2010) Russ J Struct Chem 51:288–294
21. Structure database ICSD/Retrieve 2.01 by Dr. M. Berndt
22. Belyi AS, Kiryanov DI, Smolikov MD, Zatolokina EV, Udras IE, Duplyakin VK (1994) Reac Kinet Mech Cat 53:183–189
23. Richardson JT (1989) Principles of catalyst preparation. Plenum Press, New York
24. Young VY, Williams KR (1999) J Electron Spectrosc Relat Phenom 104:221–232
25. Vlaev LT, Ivanov IvD, Damyanov DP (1993) Kinet Catal 34:147–154
26. Chupas PJ, Chapman KW, Halder GJ (2011) J Am Chem Soc 133:8522–8524
27. Chupas PJ, Chapman KW, Chen H, Grey CP (2009) Catal Today 145:213–219
28. Newton MA, Chapman KW, Thompsett D, Chupas PJ (2012) J Am Chem Soc 134:5036–5039
29. Chupas PJ, Chapman KW, Jennings G, Lee PL, Grey CP (2007) J Am Chem Soc 129:13822–13824